The Journal of Immunology

Spatial Organization of Signal Transduction Molecules in the NK Cell Immune Synapses During MHC Class I-Regulated Noncytolytic and Cytolytic Interactions

Yatin M. Vyas, Kamini M. Mehta, Margaret Morgan, Hina Maniar, Linda Butros, Steffen Jung, Janis K. Burkhardt and Bo Dupont

J Immunol 2001; 167:4358-4367; ;
doi: 10.4049/jimmunol.167.8.4358
http://www.jimmunol.org/content/167/8/4358

The Journal of Immunology is published twice each month by
The American Association of Immunologists, Inc.,
1451 Rockville Pike, Suite 650, Rockville, MD 20852

Print ISSN: 0022-1767 Online ISSN: 1550-6606.

Spatial Organization of Signal Transduction Molecules in the NK Cell Immune Synapses During MHC Class I-Regulated Noncytolytic and Cytolytic Interactions

Yatin M. Vyas,* Kamini M. Mehta,* Margaret Morgan,† Hina Maniar,* Linda Butros,* Steffen Jung,‡ Janis K. Burkhardt,† and Bo Dupont*

The cytolytic activity of NK cells is tightly regulated by inhibitory receptors specific for MHC class I Ags. We have investigated the composition of signal transduction molecules in the supramolecular activation clusters in the MHC class I-regulated cytolytic and noncytolytic NK cell immune synapses. KIR2DL3-positive NK clones that are specifically inhibited in their cytotoxicity by HLA-Cw*0304 and polyclonal human NK cells were used for conjugate formation with target cells that are either protected or are susceptible to NK cell-mediated cytotoxicity. Polarization of talin, microtubule-organizing center, and lysosomes occurred only during cytolytic interactions. The NK immune synapses were analyzed by three-dimensional immunofluorescence microscopy, which showed two distinctly different synaptic organizations in NK cells during cytolytic and noncytolytic interactions. The center of a cytolytic synapse with MHC class I-deficient target is comprised of a complex of signaling molecules including Src homology (SH)2-containing protein tyrosine phosphatase-1 (SHP-1). Closely related molecules with overlapping functions, such as the Syk kinases, SYK, and ZAP-70, and adaptor molecules, SH2 domain-containing leukocyte protein of 76 kDa and B cell linker protein, are expressed in activated NK cells and are all recruited to the center of the cytolytic synapse. In contrast, the noncytolytic synapse contains SHP-1, but is lacking other components of the central supramolecular activation cluster. These findings indicate a functional role for SHP-1 in both the cytolytic and noncytolytic interactions. We also demonstrate, in three-cell conjugates, that a single NK cell forms a cytolytic synapse with a susceptible target cell in the presence of both susceptible and nonsusceptible target cells. *The Journal of Immunology,* **2001, 167: 4358–4367.**

Natural killer cells are lymphocytes that respond to IFN-$\alpha\beta$ and IL-12 during infection by viruses and other intracellular pathogens. They represent an interface between innate and adaptive immunity by their rapid production of cytokines, such as IFN-γ and TNF-α. NK cells are also cytotoxic to certain tumor cells and virally infected cells (1). The cytolytic activity is tightly regulated by inhibitory receptors with ligand specificity for MHC class I Ags (2–4). The MHC class I-dependent regulation of NK cell cytotoxicity was first conceptualized by Ljunggren and Karre (5) as the missing self hypothesis, which states that target cell loss of self MHC class I will remove the inhibitory signals for NK cytotoxicity. The dominating NK receptors with ligand specificity for murine H-2 class I MHC Ags are the C-type lectin receptors of the Ly49 family (3, 6), while the corresponding human NK receptors belong to the Ig superfamily of molecules and are named killer cell Ig-like receptors (KIR)[3] (2–4). Other NK receptors have ligand specificity for MHC class Ib molecules: the Qa1b in the mouse and HLA-E in man (7, 8). These NK receptors are heterodimers composed of the C-type lectin molecules NKG2A and CD94. Other NK receptors, such as Ig-like transcripts have been identified, and some of these also have ligand specificity for MHC class I Ags (3, 4, 9). NK receptors for MHC class I Ags exist as pairs of inhibiting and activating receptors with highly homologous extracellular ligand binding domains. It has been shown that the inhibitory KIR and CD94/NKG2 receptors have significantly higher ligand affinity than the corresponding activating receptors (10, 11). Interactions between NK cells and autologous target cells of hemopoietic origin are dominated by the inhibitory signals preventing autocytotoxicity (2–4). Inhibitory receptors contain in their cytoplasmic domain one or more immunoreceptor tyrosine-based inhibitory motifs, which, upon tyrosine phosphorylation, recruit and activate cytoplasmic tyrosine phosphatases. NK receptors predominantly recruit the Src homology (SH)2-containing protein tyrosine phosphatase (PTP)-1 (SHP-1) (12–15). Biochemical analyses of signal transduction pathways mediated by inhibitory NK receptors have demonstrated a central role for SHP-1 in dephosphorylation of activating receptors such as 2B4 (16) and inactivation of downstream targets mediating the cytolytic granule exocytosis pathways (12–15, 17–19).

Unidirectional killing by cytolytic effector lymphocytes is known to involve accumulation of actin, talin, and cytolytic granules at the

*Immunology Program, Sloan-Kettering Institute for Cancer Research, Memorial Sloan-Kettering Cancer Center, New York, NY 10021; †Department of Pathology, University of Chicago, Chicago, IL 60637; and ‡Skirball Institute of Biomolecular Medicine, New York University Medical Center, New York, NY 10016

Received for publication January 4, 2001. Accepted for publication August 7, 2001.

The costs of publication of this article were defrayed in part by the payment of page charges. This article must therefore be hereby marked *advertisement* in accordance with 18 U.S.C. Section 1734 solely to indicate this fact.

[1] This work was supported by National Institutes of Health Grants CA08748 and CA23766.

[2] Address correspondence and reprint requests to Dr. Bo Dupont, K-406, Memorial Sloan-Kettering Cancer Center, 1275 York Avenue, New York, NY 10021. E-mail: b-dupont@ski.mskcc.org

[3] Abbreviations used in this paper: KIR, killer cell Ig-like receptor; BLCL, B lymphoblastoid cell line; BLNK, B cell linker protein; SMAC, supramolecular activation cluster; cSMAC, central SMAC; 2D, two-dimensional; 3D, three-dimensional; GEM, glycolipid-enriched microdomain; MTOC, microtubule-organizing center; NKIS, NK cell immune synapse; PLC-γ_1, phospholipase C-γ_1; PKC-θ, protein kinase C-θ; pSMAC, peripheral SMAC; PTK, protein tyrosine kinase; PTP, protein tyrosine phosphatase; SH, Src homology; SHP-1, SH2-containing PTP-1; SLP-76, SH2 domain-containing leukocyte protein of 76 kDa.

0022-1767/01/$02.00

cell-cell contact site as well as reorientation of microtubule-organizing center (MTOC) (20–24). In recent studies Ras-independent mitogen-activated protein kinase signals and phosphoinositide-3 kinase were shown to critically control lytic function and perforin/granzyme B polarization in NK-92 cells during tumor cell lysis (25, 26).

Direct analysis of signaling events in single NK cell-target cell conjugates regulated by MHC class I is limited to date. It has been shown that lipid rafts, enriched in signaling molecules, become polarized to the cell-cell contact area in NK cell conjugates with sensitive tumor cells, and this redistribution requires activation of Src and Syk kinases (27). It has also been shown that translocation of the MTOC is associated with activation of the tyrosine kinase, PYK-2 (28). In two other recent reports the inhibitory NK receptors and their corresponding MHC class I ligands were shown to colocalize in the contact area between NK cells and target cells (29, 30).

More information has been obtained from analysis of TCR-mediated signaling events in single Th cell conjugates interacting with peptide-MHC specific APCs (31, 32). It has been demonstrated that a highly structured intercellular interface, termed the supramolecular activation cluster (SMAC) (33, 34) or immunological synapse (35, 36) is formed, in which the adhesion molecule LFA-1 and the actin binding protein talin accumulate in the peripheral SMAC (pSMAC), while the TCR and the signaling molecule protein kinase C-θ (PKC-θ) were shown to cluster in the central SMAC (cSMAC) (33, 34). This structure is thought to be critical for optimizing the interactions between signaling molecules and their substrates. Although the distribution of only a small number of molecules has been reported to date, it is highly characteristic that LFA-1 and talin form a ring, which encloses TCR/MHC complexes and PKC-θ. The SMAC forms only under conditions where T cells receive a productive signal. When APCs lack peptide or when antagonistic peptide is used, no molecular segregation has been observed (34–38). Recently, in Jurkat T cell-APC conjugates, PKC-θ was shown to translocate to the membrane lipid rafts in the immune synapse (39). Furthermore, two recent studies in T cell-B cell conjugates and T cell-dendritic cell conjugates have shown an active role of the target cell in formation of the T cell immune synapse (40, 41).

In the present study we have performed an analysis of the NK cell immune synapse (NKIS) in cytolytic and noncytolytic interactions with target cells. Two different in vitro systems have been investigated. In the first system polyclonal human NK cells were used as effector cells, and an autologous EBV-transformed B lymphoblastoid cell line (BLCL) was considered the nonsusceptible target and compared with the MHC class I-deficient B cell line 721.221, which is susceptible to NK cell-mediated cytotoxicity. In the second system NK cell-target cell conjugates were analyzed using KIR2DL3-positive NK clones that in the in vitro cytotoxicity assay were noncytolytic against 721.221 transfected with HLA-Cw*0304 and were cytolytic against untransfected 721.221 targets. In the first model system all the inhibitory interactions between NK cells and MHC class I ligands are assessed simultaneously in conjugates with autologous BLCL, while none of these interactions can occur with the 721.221 target. In the second system the target cells differ for only a single HLA class I allele, which is the ligand for the inhibitory KIR molecule, KIR2DL3, present on the NK clone. In both systems the inhibition of NK cytotoxicity is lifted in the presence of anti-HLA class I mAb (42–44).

A detailed immunofluorescence analysis of the spatial recruitment of early signal transduction molecules, cytoskeletal elements, and secretory organelles in conjugates formed between NK cells and target cells was assessed. Selection of Abs for the characterization of NKIS was based on information gained from biochemical analysis of signal transduction in NK cells (12–19, 27, 45–47) and previous studies of the immune synapses formed in Ag-specific Th cell interactions with APC (33, 36–38). We anticipated that the cytolytic NKIS would have features in common with the Ag-specific T cell immune synapse. Therefore, Abs detecting Src kinases, Syk kinases, adaptor molecules, PKC-θ, and Itk were included in this analysis and expected to be present in the cytolytic cSMAC. In contrast, activation and recruitment of the cytoplasmic tyrosine phosphatase SHP-1 were expected to dominate the cSMAC in the noncytolytic NKIS. Redistribution of LFA-1 and talin into the pSMAC of the Ag-specific T cell immune synapse has been observed (33–38); therefore, Abs to these molecules were also included in the present study. Our analysis establishes that two distinctly different reorganizations occur in cytolytic and noncytolytic NKIS.

Materials and Methods

Cells

Polyclonal NK cells (i.e., NK cell lines) were generated and maintained as previously described (48). Briefly, FACS-sorted NK cells ($CD56^+$, $CD3^-$) were cocultured with irradiated allogeneic PBMC and EBV-transformed allogeneic BLCL (JY) and activated with 300 IU/ml IL-2 (provided by the National Cancer Institute/Biological Response Modifiers Program, Frederick, MD). NK clones were generated after FACS sorting for $CD56^+CD3^-$ subpopulation of lymphocytes from freshly isolated PBMC of a donor homozygous for HLA-Cw*0304. The postsort purity of NK cells was confirmed. NK cells were then plated in limiting dilution at 0.3 cells/well in 40-μl tissue culture plates (Robbins Scientific, Sunnyvale, CA). NK cell clones were cultured in IMDM (Life Technologies, Gaithersburg, MD) with 10% FCS containing heat-inactivated human AB serum (Pel-Freez Biologicals, Rogers, AR) and 300 IU/ml IL-2. The cells were cultured at 37°C in 7.5% CO_2. At the start of the culture and weekly thereafter until expanded into 48-well culture plates, the clones were cocultured with 1×10^6/ml irradiated allogeneic PBMC and 1×10^5/ml irradiated EBV-BLCL (JY). Coculturing with PBMC and BLCL-JY was discontinued once cultures were expanded into 24-well plates. All clones were then allowed to grow in 24-well plates until an adequate number of cells was reached, usually within 5–7 days. Clones were then characterized for receptor phenotype (DX9, GL183, EB6, and CD94) and used for ^{51}Cr release cytotoxicity and conjugation assays. NK clones selected for further studies were $CD3^-CD56^+$, and $GL183^+$ and mediated NK cytolytic function against 721.221 (class I-negative EBV-BLCL), but protected autologous BLCL and .221-Cw*0304 cells (self-allele transfectant). The HLA class I-negative cell line, 721.221, was used as an NK-sensitive target, while autologous BLCL and .221-Cw*0304 cells were used as an NK-protected target as previously described (42). The .221-Cw*0304 cell line was a gift from Dr. P. Parham (Stanford University, Stanford, CA). For conjugation assays, the target cells were preincubated with CellTracker Blue CMAC (Molecular Probes, Eugene, OR) for 30 min at 37°C and washed in serum-free medium before use. This allowed easy identification of target cell in an NK-target conjugate. In three cell conjugates only autologous BLCLs were prelabeled blue, and 721.221 cells were unlabeled. The 721.221 cells were identified by their large size and lack of LFA-1 staining, whereas NK cells stained for CD11a.

Antibodies

Primary. NK cells were phenotyped with anti-KIR3DL1 (DX9), anti-KIR2DL3/2DS2/2DS3 (GL183), anti-KIR2DL1/2DS1 (EB6), and anti-human CD94 mAbs, which were purchased from Immunotech (Marseilles, France). Anti-CD56 and anti-CD3 were purchased from BD Biosciences (San Jose, CA). Mouse monoclonal anti-human talin and α-tubulin (identifies tubules and MTOC) were purchased from Chemicon International (Temecula, CA) and Amersham Pharmacia Biotech (Piscataway, NJ), respectively. Goat polyclonal anti-human Itk, talin, PKC-θ, ZAP-70, mouse monoclonal anti-human phospholipase C-γ_1 (PLC-γ_1), rabbit polyclonal anti-human SHP-1, Fyn, Lck, and SYK were purchased from Santa Cruz Biotechnology (Santa Cruz, CA).

Goat anti-B cell linker protein (anti-BLNK) affinity-purified antiserum raised against the C-terminal 19 aa of human BLNK and a mouse mAb (IgG_{2a}) detecting BLNK were both used in the experiments (Santa Cruz Biotechnology). The mouse anti-BLNK Ab identifies the epitope corresponding to aa 4–205 mapping at the N terminus of BLNK of human origin. A sheep anti-human SH2 domain-containing leukocyte protein of

76 kDa (SLP-76) was a gift from Dr. G. Koretzky (University of Pennsylvania, Philadelphia, PA). Mouse anti-human LAMP-1 (H4A3; identifies lysosomes) was obtained from the Developmental Studies Hybridoma Bank, Department of Biological Sciences, University of Iowa (Ames, IA). Mouse anti-CD11a was obtained from the Monoclonal Antibody Core Facility, Sloan-Kettering Institute (New York, NY). Anti-HLA class I mAb, DX17 (IgG1) was a gift from Dr. L. Lanier (University of California, San Francisco, CA) and Dr. J. Phillips (DNAX Research Institute, Palo Alto, CA). Isotype control IgG1 Ab was purchased from BD Biosciences (Mountain View, CA). Cells were labeled with a maximum of four primary Ab combinations of mouse, rabbit, goat, and sheep.

Secondary. Affinity-purified second Abs and species-absorbed conjugates (FITC, Cy3, Cy5 (near-infrared emission), aminomethyl coumarinacetic acid (UV)) for multiple labeling were purchased from Chemicon International. CellTracker Blue CMAC and Orange CMTMR were purchased from Molecular Probes.

Western blot analysis

The presence of BLNK was assessed in NK, T, and B cells. NK cells, Jurkat T cells, and EBV-transformed B cells were washed and lysed with the lysis buffer (1% Triton X-100, 0.1% SDS, 150 mM NaCl, 5 mM EDTA, 1 mM PMSF, and 1 μg/ml leupeptin). Lysates were run on 10% SDS-PAGE. Proteins were transferred to nitrocellulose membrane (Bio-Rad, Richmond, CA), and the blots were blocked with 5% milk. Membranes probed with a 1/200 dilution of mouse anti-human BLNK mAb (Santa Cruz Biotechnology) were then washed and incubated with a 1/10,000 dilution of goat anti-mouse HRP secondary Ab (Bio-Rad). Following multiple washes the membranes were developed with ECL (NEN Life Sciences, Boston, MA). Cell lysates stained only with goat anti-mouse HRP secondary Ab were used as controls.

Flow cytometry

Analysis of NK cell conjugates using polyclonal NK cell lines and NK clones was performed on FACScan (BD Biosciences) as previously described (49). Target cells were labeled with CellTracker Orange CMTMR, and NK cells with FITC-labeled anti-CD56. Polyclonal NK cells were used to form conjugates with .221 and autologous BLCL, and NK clones were used to form conjugates with .221 and .221-Cw*0304. Aliquots of effector-target cell suspensions were removed after incubation at 37°C for 1, 3, 5, 10, 15, and 30 min and were placed on ice for immediate FACS analysis. Effectors and targets mixed in the presence of EDTA, which prevents conjugation, served as a control sample. The percentage of conjugated effector cells was determined after dividing the number of dual-labeled particles by the total number of effector lymphocytes and multiplying the result by 100 (49).

Cytotoxicity assay

Cell-killing assays were performed using polyclonal NK cells and NK clones as effectors and ^{51}Cr-labeled autologous BLCL, 721.221, and .221-Cw*0304 as targets. Assays were performed in triplicate for 4 h at an E:T ratio of 7:1. The percent specific lysis was calculated as previously described (48). Autologous BLCL and .221-Cw*0304 targets were tested in the presence (10 μg/ml) or the absence of anti-HLA class I mAb, DX17 and its isotype control Ab IgG1. DX17 is known not to induce ADCC (42–44). For cold target cell inhibition, either unlabeled autologous BLCL or 721.221 were added at increasing E:T cell ratios to ^{51}Cr-labeled 721.221.

Conjugation assay

NK cells and targets were prepared for conjugation after washing in serum-free medium and adjusting the concentration to 1×10^6/ml. Effector and target cells were mixed at an E:T cell ratio of 3:2 and spun at 500 rpm for 5 min at room temperature. For triple-cell conjugates equal numbers of autologous BLCL and .221 were mixed with NK cells. Before mixing, autologous BLCL cells were prelabeled with blue cell tracker dye while keeping .221 cells unlabeled, allowing easy identification of the two targets in the triple-cell conjugate. After incubating at 37°C for 5 min, cells were gently resuspended and transferred to poly-L-lysine-coated slides (Labscientific, Livingston, NJ), briefly cytocentrifuged, and fixed in 3% paraformaldehyde. After permeabilizing both with Triton X-100 (0.2% in PBS) for 1 min and 0.01% saponin/0.25% gelatin/0.02% NaN_3 (in PBS) for 20 min, cells were incubated with primary Abs. For visualizing cell surface molecules such as LFA-1, fixed cells were labeled before membrane permeabilization. After multiple washes with serum-free medium, cells were incubated with secondary Abs. Cells mounted with ProLong antifade kit (Molecular Probes) were then analyzed with fluorescent microscopy.

Fluorescent microscopy

In all experiments an Intelligent Imaging Innovations imaging system (Intelligent Imaging Innovations, Denver, CO) with a Zeiss Axioplan 2 microscope and AttoArc mercury light source (Zeiss, New York, NY), which includes motorized 0.1-μm linear encoders on *x*- and *y*-axes, harmonic drive *z*-focusing, Nomarski optics, motorized filter turret, a Sensicam SVGA high performance camera to record fluorescence, and differential interference contrast images, was used. Based on the Nomarski imaging, cells that were clearly conjugated were examined for their fluorescence and selected for scoring analysis using SlideBook analysis software (Intelligent Imaging Innovations). Images were obtained in both two-dimensional (2D) (*x*-*y*-axis) and in three-dimensional (3D) (*x*-*z*-axis) (34). Sixty to 70 serial optical sections of 0.1-μm thickness were acquired for each label. The digital recorded data were then deconvolved using Nearest Neighbor Deconvolution, giving the fluorescent image representative of the label in the entire cell and not just in a single plane. The contact areas (synapses) were acquired using both the mask function and the three-view function of the SlideBook software, which displays all three (*xy*, *xz*, *yz*) orthogonal planes.

Analysis of immune synapses

Based on the Nomarski images, cells that were clearly conjugated were selected for fluorescent analysis. Fifty to 70 conjugates were randomly selected for each label and target combination from two to four independent experiments. It is specifically stated in *Results* when <50 conjugates were analyzed. Two- and three-dimensional images of all such conjugates were acquired and analyzed. The scoring of the synaptic regions was made following acquisition, deconvolution, and rendering of 60–70 *z*-stack images. Such projections in the *z*-axis of the contact areas yielded three distinct patterns: 1) formation of ordered SMAC structures with peripheral and central clusters of molecules, 2) absence of the ordered SMAC structures resulting in homogenous distribution of the molecules, and 3) uninterpretable SMACs. SMAC was considered uninterpretable when the *x*-*y*-axis of the deconvolved fluorescent image was not congruous with the plane of the three-view function, thus allowing only partial visualization of the projections in the *z*-axis. Uninterpretable SMACs were observed in 14% (range, 8–20%) of the randomly selected conjugates.

Analysis of polarization event

Localization of MTOC, talin, and lysosomes in the NK-target cell conjugates was evaluated to determine the presence or absence of polarization of these organelles toward the contact site. NK cell was divided into three zones: 1) proximal one-third, as an area in the cell closest to the cell-cell contact with the target; 2) distal one-third, as an area most distant from the cell-cell contact; and 3) middle one-third, as an area in between the two zones. MTOC and lysosomes were considered polarized to the cell-cell contact when they were located in the proximal one-third of the NK cell. Any other observations, i.e., localization in the middle or distal one-third of the cell from the contact area, were considered nonpolarized events. Talin was considered polarized when it was seen to cluster at the cell-cell contact, as determined by the fluorescent intensity of the molecule being highest in the cell-cell contact area compared with the rest of the cell. Clustering of talin in any other site except the contact zone and equal distribution of talin around the cell were both considered nonpolarized events. Scoring analysis of the polarization events was performed after conducting three independent experiments with each target using either polyclonal NK cells or NK clones in conjugates with .221, .221-Cw*0304, and autologous BLCL target cells. Fifty conjugates were scored in each of the three experiments.

Results

Functional characterization of cytolytic and noncytolytic conjugates

Two experimental models were applied to analyze differences in the immune synapses during the cytolytic and noncytolytic interactions of human NK cells. In the first model polyclonal NK cells (i.e., NK cell lines) generated from healthy donors were used as effectors. The targets in this assay included the human major histocompatibility Ag (HLA) class I-negative cell line 721.221 (.221) as a susceptible target and in vitro established autologous EBV-transformed BLCL as a nonsusceptible target. As shown in Fig. 1*A*, NK cells do not mediate cytotoxicity against the autologous BLCL, while the HLA class I-deficient target .221 is susceptible to

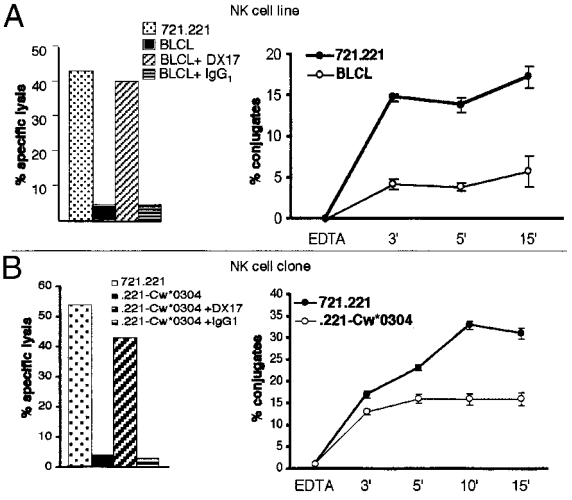

FIGURE 1. NK cytotoxicity and quantitative FACS analysis of NK conjugates. *A*, Data obtained with NK cell lines; *B*, data with NK clones. *Left*, Cytotoxicity pattern of NK cells against 721.221 and BLCL (five experiments; *a*) and 721.221 and .221-Cw*0304 (two experiments; *b*) in the presence or the absence of anti-HLA class I Ab DX17 along with the isotype IgG1 control. *Right*, Line plot with error bars (mean ± SEM) represents median percentages of conjugated NK cells with .221 and BLCL (*a*) and .221 and .221-Cw*0304 (*b*) analyzed at indicated time points (minutes) and with the EDTA control. Conjugated NK cells were determined by FACS analysis as dual-labeled particles after labeling NK cells with anti-CD56 FITC (green fluorescence) and target cells with CellTracker orange CMTMR (red fluorescence). The percentage of conjugated NK cells was calculated as described in *Materials and Methods*.

NK cell-mediated lysis. When BLCL target is tested in the presence of the anti-HLA class I mAb DX17, which does not bind to FcR (42–44), the protection against NK cytotoxicity is removed. However, this inhibition is not lifted in the presence of the isotype control Ab IgG1 (Fig. 1*A*, *left panel*) or anti-CD56 (data not shown). Therefore, the protection of autologous target is MHC class I-regulated and mediated by the inhibitory signals. Lack of cytotoxicity against autologous BLCL target cells is not due to lack of NK cell-target cell conjugate formation. Conjugates are formed both with the autologous BLCL as well as with 721.221. However, the number of conjugates formed with autologous BLCL at different time points is smaller than the number of conjugates formed with the susceptible target .221 (Fig. 1*A*, *right panel*). The differences in the number of conjugates formed with the two cell lines are not due to differences in expression of intercellular adhesion molecules ICAM-1 and -2 (data not shown). However, the origins of autologous BLCL and 721.221 target cells are different, and this could potentially account for the differences observed in the number of conjugates formed. The receptor-ligand interactions responsible for the lack of cytotoxicity against autologous BLCL are probably multiple, as are the signals that induce cytotoxicity against .221. Therefore, this model is used to identify the general differences in NKIS between cytolytic and noncytolytic conjugates.

The second in vitro model uses a well-defined inhibitory KIR interaction with the cognate HLA class I ligand. Here the effector cells are NK clones derived from a donor homozygous for the KIR2DL3 ligand, HLA-Cw*0304. NK clones that stained positively with mAb GL 183 were tested in cytotoxicity assays with .221 and .221 stably transfected with HLA-Cw*0304. NK clones that were cytotoxic against .221 but noncytotoxic against .221-Cw*0304 were selected for further analysis. The protection of .221-Cw*0304 was lifted in the presence of anti-HLA class I mAb DX17, but not in the presence of the isotype control Ab IgG1 (Fig. 1*B*, *left panel*) or anti-CD56 (data not shown). Protection of .221-Cw*0304 was also lifted with mAb GL 183 (data not shown), consistent with previous studies (42). Therefore, the ligand-receptor pair of HLA-Cw*0304 and KIR2DL3 that controls the inhibition of NK cytotoxicity is directly tested in this model system. The number of conjugates formed with the nonsusceptible target, .221-Cw*0304, was fewer than the number obtained with the susceptible target, .221 (Fig. 1*B*, *right panel*), which is similar to the findings made in the first model (Fig. 1*A*, *right panel*). A higher number of conjugates was formed at each time point using NK clones compared with polyclonal NK cells (Fig. 1, *right panels*).

Cytoskeletal remodeling and polarization events in the cytolytic and noncytolytic conjugates

Conjugates with the susceptible and nonsusceptible target cells using polyclonal NK cell lines and NK clones were analyzed for localization of MTOC and lysosomes (cytolytic granules) (22, 23) as well as the clustering of actin and talin. The data in Fig. 2 are representative of 150 conjugates analyzed for each label and target combination. Conjugates formed using the polyclonal NK cell line that is cytotoxic for .221 and noncytotoxic for autologous BLCL were initially analyzed. Polarization toward .221 cells was observed for the MTOC in 80% (n = 78–82), lysosomes in 78% (n = 76–80), and talin in 75% (n = 70–78) of the conjugates (Fig. 2, *second row*). The results for redistribution of actin and talin were similar (data not shown). In contrast, <25% (n = 18–30) of NK cell conjugates showed polarization of any of these elements toward autologous BLCL targets (Fig. 2, *first row*). In the second dataset conjugates formed using GL183$^+$ NK clones that are cytotoxic to .221 and noncytotoxic to .221-Cw*0304 were analyzed. Here, polarization toward .221 cell was observed for the MTOC in 84% (n = 82–86), lysosomes in 80% (n = 78–82), and talin in 78% (n = 75–80) of the conjugates (Fig. 2, *third row*). In contrast, <20% (14–25) of NK cell conjugates showed polarization of any of these elements toward .221-Cw*0304 target cells (Fig. 2, *fourth row*). Therefore, conjugates with autologous BLCL and .221-Cw*0304 expressing a single self HLA-Cw allele gave similar results in cortical cytoskeletal remodeling and polarization events in both polyclonal NK cells and NK clones. These results demonstrate that inhibitory signaling does not require large scale remodeling of the cortical cytoskeleton, nor does it involve changes in cytoplasmic structures normally associated with activation of the cytolytic machinery.

Distribution of signaling molecules in NK cells

To address whether the signaling molecules do or do not passively move along with the MTOC in the conjugates, the IL-2-activated NK cells were dual-labeled with Abs against a variety of signal transduction molecules and α-tubulin. Dual-labeling with closely related molecules such as the two Syk kinases, SYK and ZAP-70, and two adaptor molecules, SLP-76 and BLNK, was also evaluated to study the possible redundancy of such molecules in NK signaling. Digital immunofluorescence microscopy was used to acquire fluorescent images keeping MTOC and the labeled molecule in the same focal plane. The data in Fig. 3 are representative of 20 NK cells analyzed for each Ab combination. The distribution of signaling molecules in relation to MTOC was different for each molecule. The distribution of SHP-1 and SLP-76 was distinct from the location of MTOC (in green, Fig. 3, *rows 3* and *4*). Lck, ZAP-70, BLNK, Itk, and PKC-θ have some portion of their molecules that colocalize with MTOC (in yellow, Fig. 3, *panels 1*, *2*, *5*, *6*, and *7*, overlay). These results indicate that at least a subset of some of the signal transduction molecules colocalizes with MTOC. Therefore, they may be translocated with MTOC to the contact site with

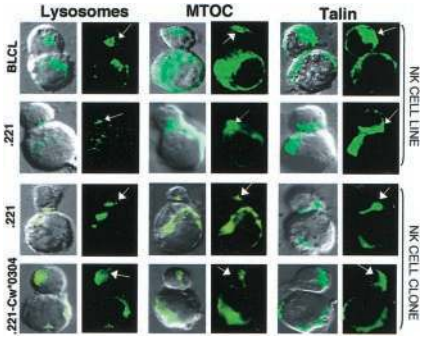

FIGURE 2. Cortical cytoskeletal and cytoplasmic organelles. NK conjugates using NK cell lines (*top two rows*) and NK clones (*bottom two rows*) are shown. Conjugates with autologous BLCL (*top row*), .221(*middle two rows*), and .221-Cw*0304 (*bottom row*) were single-labeled with Abs for lysosomes (*left two columns*), MTOC (*middle two columns*), and talin (*right two columns*). For each panel, an overlay of Nomarski and fluorescent fields along with the corresponding fluorescent image of the conjugate is shown. Arrows indicate the location of most intense label within the NK cell. Each picture is representative of >70% of 50 conjugates observed in each of three independent experiments.

susceptible targets similar to recent findings observed for the tyrosine kinase PYK 2 (28). It is also possible that the molecules colocalized with MTOC exist as preformed complexes in IL-2-activated NK cells. Furthermore, NK cells have closely related signaling molecules that otherwise are predominantly expressed in either B cells (e.g., BLNK and SYK) or T cells (e.g., SLP-76 and ZAP-70). The presence of BLNK was confirmed by Western blot analysis, in which an appropriate size band (68 kDa) was detected in human NK cells and EBV-transformed B cells, but not in Jurkat T cells (Fig. 4). Cellular localization of the signaling molecules was also determined. In activated NK cells the distributions of

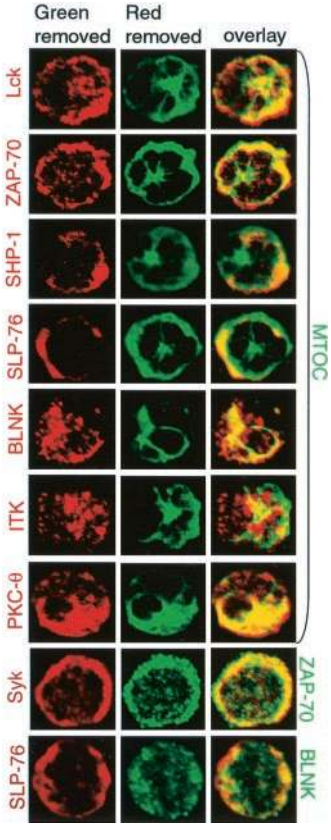

FIGURE 3. MTOC and signaling molecules. Distribution of fluorescence of signaling molecules in relation to the location of MTOC is shown. NK cells were dual-labeled for α-tubulin to show the location of MTOC (in green, *top seven rows*) and the indicated signaling molecules (in red) or with pairs of related signaling molecules (*bottom two rows*). Color-coded letters denotes combinations of Ab labels. Each Ab label is shown independently after removing either the green color (*left column*) or the red color (*middle column*) and as an overlay of two colors (*right column*). Overlapping red and green labels are seen as yellow. Twenty NK cells were analyzed for each label, and representative fluorescence patterns are shown.

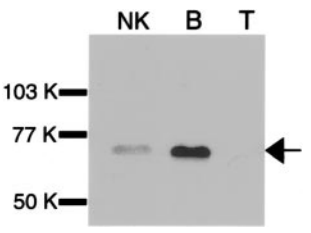

FIGURE 4. Western blot analysis of BLNK in lymphocytes. BLNK expression in IL-2-activated human NK cells, EBV-B cells, and Jurkat T cells. Western blots of whole cell lysates with mAb to human BLNK demonstrate a 68-kDa band in NK and B cells. The arrow denotes the 68-kDa band for human BLNK. The markers (kilodaltons) are shown on the *left*.

Lck, ZAP-70, and SYK were similar, having both cytoplasmic and perimembraneous localizations (in red, Fig. 3, *rows 1*, *2*, and *8*). SHP-1 and SLP-76 have predominantly perimembraneous localization (in red, Fig. 3, *rows 3* and *4*), whereas BLNK, Itk, and

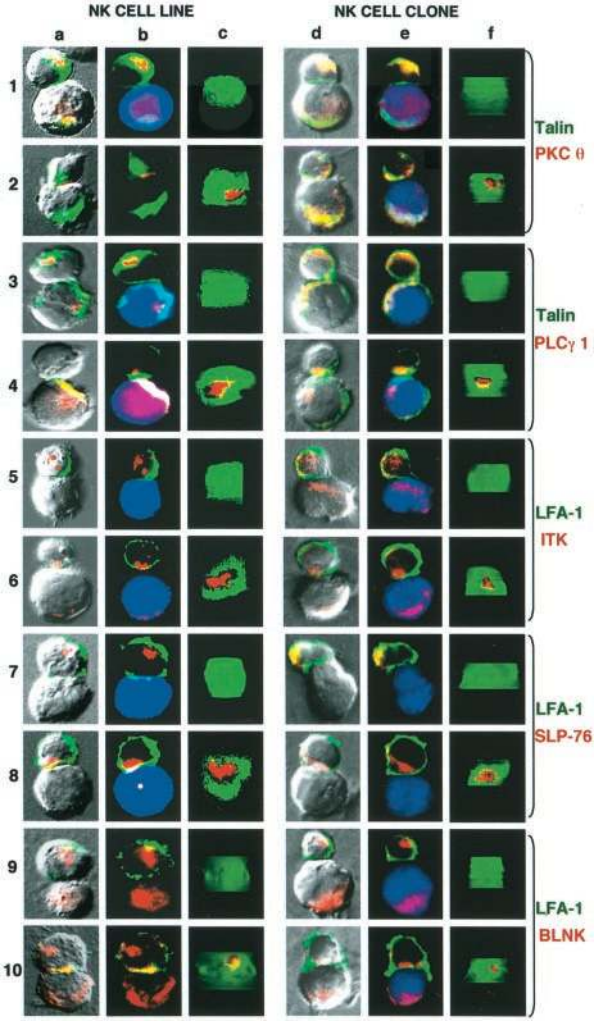

FIGURE 5. NKIS. NK cell conjugates using either NK cell lines (*column a–c*) or NK clones (*columns d–f*) are shown. Conjugates with autologous BLCL (*panels 1*, *3*, *5*, *7*, and *9*, *a–c*), .221 (*panels 2*, *4*, *6*, *8*, and *10*, *a–f*), and .221-Cw*0304 (*panels 1*, *3*, *5*, *7*, and *9*, *d–f*) are shown as an overlay of Nomarski and fluorescent fields (*columns a* and *d*), multicolored fluorescent image (*columns b* and *e*), and projections in the *z*-axis of the NK-target contact area (*columns c* and *f*). In a conjugate, NK cell is the *top* cell, and the target cell is the *bottom* cell. Conjugates were dual-labeled with the indicated Ab pairs (color-coded letters). The target cell is shown in blue (all panels except *2b*, *9b*, and *10b*). Each set of three pictures is representative of 75–80% of 50–70 conjugates analyzed for each Ab and target combination obtained in at least two independent experiments (see *Materials and Methods* for further details).

PKC-θ have predominantly cytoplasmic localization (in red, Fig. 3, *rows 5–7*). Although, SYK and ZAP-70 have mostly overlapping distribution (in yellow, Fig. 3, *row 8*, overlay), there are areas where the two molecules are not colocalized.

Cytolytic and noncytolytic NKIS

NKIS visualized as projections in the *z*-axis were analyzed using the 3D digital immunofluorescence microscopy. The word synapse is used to describe structures visualized in 3D (*x*-*z*-axis) and not in 2D (*x*-*y*-axis) fluorescent images (34). In the figure the fluorescent distributions of the signaling molecules are shown to be discrete and clumped, as the panels represent only the most intense signals within the NK cell obtained following deconvolution of 60–70 images. In one set of experiments analysis of the immune synapses was made in conjugates between polyclonal NK cells and either .221 or autologous BLCL (Fig. 5, *a–c*), and in the other set of experiments conjugates between NK clones and either .221 or .221-Cw*0304 (self allele) were analyzed (Fig. 5, *d–f*). The results of synaptic molecular redistribution obtained in both experimental models were similar. Data in the figure represent 75–80% of 50–70 conjugates analyzed for each Ab and target combination obtained in at least two independent experiments (see *Materials and Methods*). Recruitment to the immune synapse of the signaling molecules, PKC-θ, PLC-γ_1, Itk, and SLP-76, which are expected to be involved in the granule exocytosis activation pathways, was evaluated. BLNK was selected to determine the involvement of other adaptor molecules in NK signaling (50, 51). LFA-1 and components of the cortical cytoskeleton, actin and talin, are known to mediate essential functions during T cell interactions with target cells and APCs and to accumulate at the contact sites (35). Here we demonstrate that talin is clustered at the contact site with the susceptible target (i.e., .221) as seen in 2D fluorescent images (Fig. 5, *panels 2* and *4*, *b* and *e*) and is also redistributed in the cytolytic synapses (3D images) of both NK cell lines (Fig. 5, *panels 2* and *4c*) and NK clones (Fig. 5, *panels 2* and *4f*). LFA-1 did not cluster at the cell-cell contact of the cytolytic conjugates when analyzed as 2D images (Fig. 5, *panels 6*, *8*, and *10*, *b* and *e*); however, there was a distinct redistribution of LFA-1 in the cytolytic synapses (3D images), similar to that observed for talin (Fig. 5, *panels 6*, *8*, and *10*, *c* and *f*). Both LFA-1 and talin are localized in the periphery of the synapse (pSMAC), while PKC-θ (Fig. 5, *panel 2*, *c* and *f*), PLC-γ_1 (Fig. 5, *panel 4*, *c* and *f*), Itk (Fig. 5, *panel 6*, *c* and *f*), SLP-76 (Fig. 5, *panel 8*, *c* and *f*) and BLNK (Fig. 5, *panel 10*, *c* and *f*) are localized in the center (cSMAC). In contrast, redistribution in the noncytolytic immune synapse of these molecules was not observed with either autologous BLCL (Fig. 5, *panels 1*, *3*, *5*, *7*, and *9c*) or .221-Cw*0304 (Fig. 5, *panels 1*, *3*, *5*, *7*, and *9f*). This demonstrates that cytolytic effector function is associated with dramatic changes in the plasma membrane at the contact sites between NK cells and susceptible targets and can be visualized in 3D images of the projections in the *x*-*z*-axis.

Protein tyrosine kinases (PTKs) in cytolytic and noncytolytic conjugates

The early recruitment of PTKs, such as the Src kinases Lck and Fyn, and the Syk kinases SYK and ZAP-70, was visualized in cytolytic and noncytolytic NK cell conjugates formed between polyclonal NK cells and either .221 or autologous BLCL and analyzed after 10 min of NK cell-target cell mixing. The data in Fig. 6 represent 75–80% of 50–70 conjugates analyzed collectively from two to four independent experiments for each Ab and target combination. Analysis of the immune synapses in cytolytic interactions with .221 showed all four PTKs as well as BLNK to be clustered in the center of the synapse (cSMAC) surrounded by LFA-1, which is localized in the pSMAC (Fig. 6, *panels 1–3C*). It was also demonstrated by independent visualization of signaling molecules obtained after removing either red or blue colors that there was some compartmentalization within the cytolytic cSMAC. Further studies including fluorescence resonance energy transfer will be needed to address issues regarding colocalization and coassociation of molecules in the immune synapses. Recruitment to the synapse of the PTKs or adaptor proteins is not identified in NK cell conjugates with autologous cells or with .221-Cw*0304 (data not shown).

SHP-1 in cytolytic and noncytolytic conjugates

Biochemical analysis of signal transduction events mediated by inhibitory NK receptors for MHC class I Ags have clearly demonstrated that SHP-1 is recruited to these receptors and activated by a tyrosine phosphorylation-dependent mechanism (12–15, 52). Therefore, localization of SHP-1 in cytolytic and noncytolytic conjugates was determined. Experiments were performed using both model systems. In one experimental system .221 and autologous BLCL were used as targets for polyclonal NK cells, and in the other .221 and .221-Cw*0304 were used as targets for GL183$^+$NK clones. Fifty conjugates were collectively analyzed from two to four independent experiments for each Ab and target combination. The results obtained from the analysis of cytolytic conjugates with either .221 targets and NK cell lines or .221 targets and NK clones are representative of 85–90% of the conjugates (Fig. 7*A*, *top row*). It is demonstrated that SHP-1 and ZAP-70 are recruited to the cell-cell contact site with .221 (Fig. 7*A*, *b* and *e*, *top row*) and are clustered in the cytolytic cSMAC (Fig. 7*A*, *c* and *f*, *top row*). This is further demonstrated in a detailed four-color analysis of NK cell conjugates, where SHP-1 is recruited to the contact area with .221 target cells in the cytolytic conjugate (Fig. 7*B*, *a–e*). Here, SHP-1 is seen to occupy a central position along with ZAP-70 and SLP-76 at the cell-cell contact site (Fig. 7*B*, *a–e*).

Recruitment of SHP-1 to the NK cell-target cell synapse could not be identified in the majority of noncytolytic conjugates with either autologous BLCL or .221-Cw*0304 target cells analyzed 10 min after NK cell-target cell mixing. However, there is a well-defined rearrangement at the synapse (*x*-*z*-axis, 3D image) in 32% of conjugates with BLCL (16 of 50) and 40% of conjugates with .221-Cw*0304 (20 of 50 conjugates) analyzed at 10 min. Here, SHP-1 alone is recruited to the cell-cell contact site (*x*-*y*-axis, 2D image; Fig. 7*A*, *b* and *e*, *bottom row*, and Fig. 7*Bg*) and is clustered in the cSMAC, while LFA-1 is redistributed in the pSMAC of the noncytolytic NKIS (Fig. 7*A*, *c* and *f*, *bottom row*, and Fig. 7*Bg*, *inset*). Although only 32–40% of the noncytolytic conjugates demonstrated cSMAC with SHP-1, the other conjugates did not demonstrate any redistribution of LFA-1 in the synapse when analyzed at 10 min of conjugate formation. In contrast to cytolytic conjugates formed with HLA class I-deficient target cells, SHP-1 was not associated with ZAP-70 or SLP-76 in the noncytolytic conjugates formed with either autologous BLCL or .221-Cw*0304, as demonstrated by absence of any other molecules in the cSMAC after removing the red color of SHP-1 (Fig. 7*A*, *c* and *f*, *bottom row*). This is also illustrated in the four-color immunofluorescence image of a noncytolytic conjugate, where SLP-76 and ZAP-70 are located in the distal one-third of the NK cell (Fig. 7*B*, *f–h*). This analysis demonstrates that noncytolytic NK cell interactions with autologous target cells involve the generation of an inhibitory immune synapse, which is dominated by SHP-1, while downstream signaling molecules are excluded from the contact region. Our results also implicate a role for SHP-1 in cytolytic NK interactions.

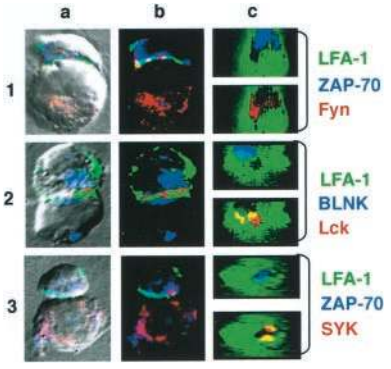

FIGURE 6. Redistribution of Src and Syk kinases in the immune synapse. Polyclonal NK cells were used to form conjugates with .221 cells. Conjugates triple-labeled with the indicated Ab combinations (color-coded letters) are shown as an overlay of Nomarski and fluorescent fields (*column a*), corresponding fluorescent image (*column b*), and projections in the *z*-axis of the contact area (*column c*), with either blue or red label removed. The data represent 75–80% of 50–70 conjugates analyzed collectively from two to four independent experiments for each Ab and target combinations.

Unidirectional interactions in triple-cell conjugates

The ability of NK cells to identify a susceptible target in the presence of a nonsusceptible target and deliver a unidirectional cytolytic hit was examined in both the cold target inhibition assay and the analyses of the three-cell conjugates. The specificity for .221 cytotoxicity is demonstrated by cold target cell inhibition, where a 100-fold excess of autologous BLCL is needed before any reduction in cytotoxicity occurs, suggesting that NK cells, even in the presence of an overwhelming number of autologous target cells, identify and lyse susceptible target cells. Furthermore, NK cells also lyse susceptible target cells (i.e.,721.221) when preincubated with autologous target cells (i.e., BLCL) for 1, 2, and 3 h (data not shown). In contrast, only a 10-fold increase in .221 cold target cells is sufficient for inhibition of ^{51}Cr-labeled 721.221 cells (Fig. 8*A*), probably due to competition between ^{51}Cr-labeled and unlabeled 721.221 target cells.

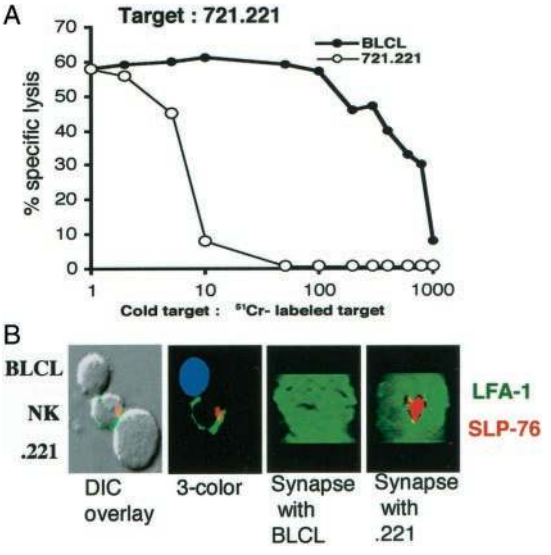

FIGURE 8. Cold target cell inhibition and triple-cell conjugates. *A*, NK cells used as effectors in a cold target inhibition assay with increasing numbers of unlabeled (cold) BLCL and .221 added to ^{51}Cr-labeled .221. *B*, One NK-two target cell (BLCL and .221) conjugates triple-labeled with the indicated Ab pair (color-coded letters) and blue cell tracker dye are shown as an overlay of Nomarski and fluorescent images, corresponding three-color fluorescence and projections in the *z*-axis of the contact areas with the *top* cell (BLCL) and the *bottom* cell (.221). The locations of the NK cell and the target cell in the conjugate are indicated on the *left* of the panel. BLCL is shown in blue, and the larger .221 cell is unlabeled.

The regulated processes that mediate such unidirectional induction of cytolytic granule exocytosis were investigated in NK cell conjugates in which one NK cell interacts with .221 and autologous BLCL simultaneously. Thirty triple-cell conjugates were analyzed after triple labeling with blue tracker dye, LFA-1 and SLP-76 (see *Materials and Methods*). The data in the figure were observed in 25 of 30 three-cell conjugates analyzed. NK cells in such conjugates demonstrate unidirectional polarization of SLP-76

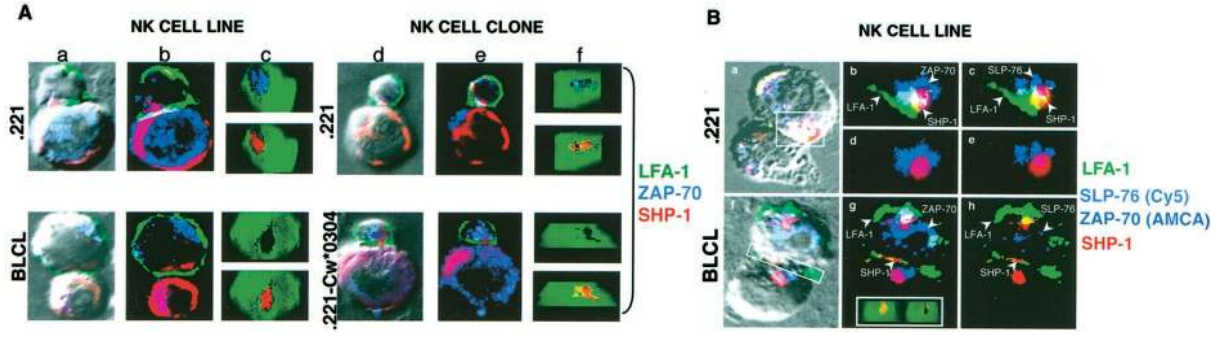

FIGURE 7. Recruitment of SHP-1 to the immune synapses. *A*, NK conjugates using NK cell lines (*left panel*) or NK clones (*right panel*) with .221 (*top row*, *a–f*), BLCL (*bottom row*, *a–c*), and .221-Cw*0304 (*bottom row*, *d–f*) triple-labeled with indicated Ab combinations (color-coded letters) are shown as an overlay of Nomarski and fluorescent fields (*columns a* and *d*), corresponding fluorescent images (*columns b* and *e*) and projections in the *z*-axis of the contact area (*columns c* and *f*), with either blue or red label removed. *B*, An NK cell line was used to form conjugates with .221 (*top row*) and BLCL (*bottom row*). Conjugates with .221 (*a–e*) or BLCL (*f–h*) were quadruple-labeled with LFA-1 (FITC, green), SLP-76 (Cy5, blue), ZAP-70, aminomethylcoumarinacetic acid (AMCA), blue), and SHP-1 (Cy3, red). The NK cell is the *top* cell in the conjugate. Fluorescent images of the multimolecular signaling complex in the boxed area (*a*) are shown (*b* and *c*) and with green color removed (*d* and *e*) along with overlay of Nomarski and fluorescent fields (*a*). In the conjugate with BLCL, overlay of Nomarski and fluorescent fields (*g*) is shown in image *f*. Note the polarization of SHP-1 (red, *f–h*), but not of ZAP-70 (blue, *f* and *g*) or SLP-76 (blue, *h*). A projection in the *z*-axis of the contact area with BLCL is shown (*inset, g*). Ab labels are indicated with arrowheads. Overlapping distributions of labels results in yellow (red and green), pink (red and blue), and white (red, green, and blue) colors. *A*, with .221 target cells, is representative of 85–90% of 50 conjugates collectively analyzed from two to four independent experiments for each Ab and target combination with NK cell lines and NK clones. Data in *A* with BLCL and .221-Cw*0304 targets are representative of a subset of conjugates. *B*, Selected conjugates that allowed representation of four-color images. The *top panel* is representative of the cytolytic NK conjugate. The *bottom panel* is representative of ~30% of noncytolytic conjugates.

only toward .221 (Fig. 8*B*, lower cell in differential interference contrast overlay and three-color image). Here, SLP-76 clusters in the cSMAC of the NK cell-contacting membrane with .221, while this was not observed in the contacting membrane with autologous BLCL (Fig. 8*B*). Triple-cell conjugates formed between a single NK cell and two susceptible target cells demonstrate different patterns dependent upon the indicator used for assessment of recognition and the induction of cytotoxicity. SLP-76 and PKC-θ were polarized toward only one of the two targets; in contrast, talin was polarized toward both target cells (data not shown).

Discussion

We have analyzed, at the single-cell level, the composition of signal transduction molecules in the SMACs in the MHC regulated cytolytic and noncytolytic NKIS. The NKIS were analyzed by 3D immunofluorescence microscopy for the presence or absence of several signal transduction molecules, including PTKs, a PTP, adaptor molecules, PKC-θ and PLCγ_1, in the immune synapse, and for synaptic redistribution of LFA-1 and the actin-associated molecule, talin. Two different in vitro models yielded similar results. It is demonstrated that two distinctly different NKIS can be defined: the inhibitory NKIS and the cytolytic NKIS.

The inhibitory NKIS is formed when polyclonal IL-2-activated NK cells form conjugates with autologous BLCL or when KIR2DL3-positive NK clones interact with .221 cells expressing the cognate ligand HLA-Cw*0304. When the target cell lacks self MHC, a cytolytic NKIS is formed at the contact site with the target cell. Here, the NK-target cell contact area assembles into topologically and spatially distinct regions characterized by redistribution of LFA-1 and talin in the pSMAC, and a multimolecular signaling complex including SHP-1 is assembled in the cSMAC. In contrast, the inhibitory NKIS is characterized by redistribution of LFA-1 in the pSMAC and clustering of only SHP-1 in the cSMAC. The cytolytic NKIS has several features in common with the TCR-specific immune synapse observed for Th lymphocytes interacting with their Ag-specific APCs (34–38).

Visualization of the signaling molecules included in the cytolytic cSMAC provides further insight into the spatial organization of enzymes and adaptor molecules needed for initiation of cytolytic effector function. Translocation of signaling molecules from the cytosol to the NK cell plasma membrane occurs within a limited region of contact with the target cell. The complex consists of Src kinases, Syk kinases, the Tec kinase Itk, adaptor molecules, PKC-θ, and PLC-γ_1. These findings are consistent with expectations derived from biochemical analysis of receptor-mediated signaling pathways in lymphocytes (12–19, 27, 45–47, 50–55). Although the molecular basis for NKIS formation and its function remains to be defined, recent studies have suggested that the compartmentalization of the plasma membrane imposed by glycolipid-enriched microdomains (GEMs) is essential for TCR-mediated signaling (56). GEMs are enriched in molecules involved in signal transduction, such as the PTKs Lck and Fyn and the transmembrane adaptor linker of activation in T cells (57). In contrast, the PTPs CD45, SHP-1, and SHP-2 are excluded from the GEMs (58), and such restricted distribution of PTPs may play a critical role in the initiation of signaling.

Our results on clustering of the GEM-resident PTKs in the cSMAC of the cytolytic conjugates are consistent with a model in which aggregated GEMs get reorganized during cell-mediated cytotoxicity (27). We also demonstrate that SLP-76 in the cytolytic interaction is brought to the contact area in such a way that it could provide the scaffold where Itk (54), PKC-θ (55), and PLC-γ_1 (17–19) are brought in contact with their substrates (Fig. 7, *A–E*). Therefore, clustering of this activation signaling complex to the cytolytic NKIS could occur by recruitment to the GEM-resident anchoring molecule, linker of activation in T cells (51), which is tyrosine phosphorylated in cytolytically active NK cells (19). Given that the majority of SHP-1 in T cell membranes is present outside the lipid rafts (58), it was surprising to find SHP-1 in the cytolytic NKIS as a component of the multimolecular signaling complex in the cSMAC. However, it has been shown in Jurkat T cell lines that the predominantly cytosolic SHP-1 becomes enriched in membranes and GEMs in association with activated Lck (58). Therefore, it is possible that the activated Lck recruited to cytolytic NKIS will also recruit SHP-1 to GEMs. Our analysis cannot determine whether SHP-1 is present in the complex as an active enzyme. In this case SHP-1 could provide a regulatory function by guiding tyrosine phosphorylation-dependent pathways toward granule exocytosis and deactivation of signals that could mediate apoptosis or cell proliferation via regulation of mitogen-activated protein kinases (25, 26, 59). Direct support for involvement of enzymatically active SHP-1 in cytolytic NK cell effector function with MHC class I negative targets has recently been provided by studies in mice transgenic for dominant-negative SHP-1. Such mice display decreased NK cytotoxicity against MHC class I-negative targets (60).

Visualization of NK cell interactions with target cells expressing self HLA class I ligands for inhibitory NK receptors clearly demonstrates that the cytolytic effector mechanisms are not being activated. MTOC, lysosomes, and talin are not polarized to the contact site with the target (Fig. 2), and the cascade of signaling events is interrupted early in such interactions (this study and Ref. 16). This deactivation of NK cell effector functions is mediated by the interactions of inhibitory NK receptors for MHC class I, as evidenced by the occurrence of cytotoxicity in the presence of anti-HLA class I mAb (Fig. 1, *A* and *B*, *left panels*). It has recently been shown that inhibitory KIR or CD94/NKG2 receptors interacting with cognate MHC class I ligand interrupt tyrosine phosphorylation of the activating NK receptor 2B4 (16). The inhibitory NKIS has a well-defined pSMAC containing LFA-1, and a cSMAC containing only SHP-1. Recruitment and activation of SHP-1 are tyrosine phosphorylation dependent (12–15, 52). The initial NK cell activation will induce Src kinase-mediated tyrosine phosphorylation (16), and activation of SHP-1 will then occur when the inhibitory NK receptor is recruited into the synapse as a consequence of cognate MHC-ligand interactions. The perimembraneous components of Lck and SHP-1 would favor rapid initiation of the inhibitory signal transduction pathway. This could then facilitate interruption of the cytolytic signaling cascade, which also depends on Src kinase activation.

Noncytolytic NK cell conjugates were analyzed at 10 min following effector cell-target cell mixing. The majority of these conjugates display a synaptic region with uniform distribution of LFA-1 and absence of SHP-1. It is possible that these conjugates represent cell-cell interactions where the self recognition process has been completed. This conclusion is supported by recent studies in T cells, where the dephosphorylation of proteins by SHP-1 and SHP-2 was completed within 5 min of incubation of the T cell membrane with ATP and SHP-1 (58). This hypothesis is further supported by three recent studies, one demonstrating down-regulation of integrin function upon inhibitory KIR interactions with cognate HLA-C molecules (61) and the others demonstrating redistribution of inhibitory Ly49 and KIR molecules on NK cells during interactions with their ligands on target cells (29, 30). Therefore, our analyses of noncytolytic NKIS support the results obtained in the other study where the inhibitory signals initiated by KIRs block aggregation and polarization of GEMs in an SHP-1-dependent manner (27).

Our studies also demonstrate that the NK cells express signaling molecules characteristic for both T cell and B cell lineages. The two Syk kinases, ZAP-70 and SYK, which have close functional similarity (62), were recruited into the cSMAC of cytolytic NKIS (Fig. 6). The two adaptor molecules, SLP-76 and BLNK, were also recruited into the cSMAC of cytolytic NKIS. It has recently been suggested that these adaptor molecules have overlapping, yet unique, additional functions (50, 51, 63). It has previously been reported that BLNK is not present in human lymphokine-activated killer cells (64). However, our studies with two different anti-BLNK Abs, including Western blot analysis of purified IL-2 activated human NK cells and NK clones did indicate the presence of this adaptor molecule in NK cells (Fig. 4). The immunofluorescence staining in NK cells of BLNK and SLP-76 demonstrate different patterns (Fig. 3), further supporting that the Abs do not cross-react between these two molecules. In another recent report SLP-76 and BLNK were both expressed in murine macrophages and were linked to signaling via Fcγ receptors (65). Our observation that a fraction of Lck, ZAP-70, BLNK, Itk, and PKC-θ colocalized with MTOC in IL-2-activated NK cells (Fig. 3, *rows 1*, *2*, *5*, *6*, and *7*) suggest that these signaling molecules might be translocated along with MTOC to the contact area with target cells during initiation of the cytolytic signaling cascade. The recent finding of PYK-2 association and cotranslocation with MTOC in cytolytic NK effector function supports this model for temporal and spatial regulation of cytotoxicity (28).

The ability of NK cells to distinguish self from nonself based on the presence or absence of autologous MHC class I Ags on target cells was clearly illustrated in triple-cell conjugates (Fig. 8). A single NK cell interacting simultaneously with an autologous and an MHC class I-deficient target cell displays a unidirectional cytolytic immune synapse with only the class I-negative target cell (Fig. 8*B*, compare two *right side* images). The ability of an NK cell to precisely direct its cytolytic machinery toward a susceptible target when surrounded by overwhelming numbers of self targets is also illustrated in the cold target inhibition assay (Fig. 8*A*). These findings are in agreement with previous studies in cytolytic T cells (21) and with recent studies applying video microscopy of murine NK cell interactions with target cells (66). Collectively, these results support the hypothesis that the inhibitory signals within a single NK cell are spatially and temporally restricted and are limited to interactions with nonsusceptible, resistant target cells. This localized inhibition does not lead to a general inactivation of the cytolytic effector function of the cell (Fig. 8). However, a more detailed analysis of triple-cell conjugates between a single effector cell and two susceptible target cells, two effector cells and a single susceptible target cell, and other permutations is needed to dissect the directional events required for induction of cytotoxicity and simultaneous protection of self targets. We observed polarization of talin toward two susceptible targets (2D analysis, *x*-*y*-axis) interacting simultaneously with a single effector cell, but the reorganized cytolytic NKIS with PKC-θ in the cSMAC was only observed for one of the two susceptible target cells. We have not attempted to quantitate polarization of LFA-1 and/or ICAM-1 in cytolytic or noncytolytic conjugates. Previous studies of triple-cell conjugates between a single T cell and two APCs have demonstrated accumulation of ICAM-1 at the contact sites of both APCs (67).

Our studies with IL-2-activated NK cells and NK clones have been limited to a single 10 min point. Others previously reported a temporal distribution of LFA-1 in the NKIS with central accumulation of LFA-1 (29). However, this study was performed with the CD28-positive NK-like cell line, YT, where induction of the cytolytic effector function depends on signals mediated by both CD28 and LFA-1/ICAM-1 (68, 69). Sequential analysis of the NKIS with simultaneous determination of localization of NK receptors, their ligands, and signaling molecules will provide further insight into the molecular mechanisms responsible for NK cell recognition of self vs nonself.

Acknowledgments

We thank Dr. Gary Koretzky, (University of Pennsylvania, Philadelphia, PA) for the Sheep anti-human SLP- 76 and Dr. L. Lanier (University of California, San Francisco, CA) and Dr. J. Phillips (DNAX Research Institute, Palo Alto, CA) for the anti-HLA class I mAb, DX17. The mouse anti-human LAMP-1 (H4A3) was obtained from the Developmental Studies Hybridoma Bank developed under the auspices of the National Institute of Child Health and Human Development and maintained by The University of Iowa, Department of Biological Sciences, Iowa City, IA. We also thank Dr. Dan R. Littman (New York University-Skirball Institute, New York, NY) for advice and access to digital fluorescence microscope with SlideBook software. Dr. Michael Dustin (New York University-Skirball Institute, New York, NY) for helpful comments on the manuscript and Ali McBride for assistance with microscope.

References

1. Biron, C. A., K. B. Nguyen, G. C. Pien, L. P. Cousens, and T. P. Salazar-Mather. 1999. Natural killer cells in antiviral defense: function and regulation by innate cytokines. *Annu. Rev. Immunol. 17:189.*
2. Moretta, A., C. Bottino, M. Vitale, D. Pende, R. Biassoni, M. C. Mingari, and L. Moretta. 1996. Receptors for HLA class-I molecules in human natural killer cells. *Annu. Rev. Immunol. 14:619.*
3. Lanier, L. L. 1998. NK cell receptors. *Annu. Rev. Immunol. 16:359.*
4. Long, E. O. 1999. Regulation of immune responses through inhibitory receptors. *Annu. Rev. Immunol. 17:875.*
5. Ljunggren, H. G., and K. Karre. 1990. In search of the 'missing self:' MHC molecules and NK cell recognition. *Immunol. Today 11:237.*
6. Karlhofer, F. M., R. K. Ribaudo, and W. M. Yokoyama. 1992. MHC class I alloantigen specificity of Ly-49$^+$ IL-2-activated natural killer cells. *Nature 358:66.*
7. Braud, V. M., D. S. Allan, C. A. O'Callaghan, K. Soderstrom, A. D'Andrea, G. S. Ogg, S. Lazetic, N. T. Young, J. I. Bell, J. H. Phillips, et al. 1998. HLA-E binds to natural killer cell receptors CD94/NKG2A, B and C. *Nature 391:795.*
8. Vance, R. E., J. R. Kraft, J. D. Altman, P. E. Jensen, and D. H. Raulet. 1998. Mouse CD94/NKG2A is a natural killer cell receptor for the nonclassical major histocompatibility complex (MHC) class I molecule Qa-1(b). *J. Exp. Med. 188: 1841.*
9. Colonna, M., F. Navarro, T. Bellon, M. Llano, P. Garcia, J. Samaridis, L. Angman, M. Cella and M. Lopez-Botet. 1997. A common inhibitory receptor for major histocompatibility complex class I molecules on human lymphoid and myelomonocyte cells. *J. Exp. Med. 186:1809.*
10. Winter, C. C., J. E. Gumperz, P. Parham, E. O. Long, and N. Wagtmann. 1998. Direct binding and functional transfer of NK cell inhibitory receptors reveal novel patterns of HLA-C allotype recognition. *J. Immunol. 161:571.*
11. Vales-Gomez, M., H. T. Reyburn, R. A. Erskine, M. Lopez-Botet, and J. L. Strominger. 1999. Kinetics and peptide dependency of the binding of the inhibitory NK receptor CD94/NKG2-A and the activating receptor CD94/NKG2-C to HLA-E. *EMBO J. 18:4250.*
12. Burshtyn, D. N., A. M. Scharenberg, N. Wagtmann, S. Rajagopalan, K. Berrada, T. Yi, J. P. Kinet, and E. O. Long. 1996. Recruitment of tyrosine phosphatase HCP by the killer cell inhibitor receptor. *Immunity 4:77.*
13. Campbell, K. S., M. Dessing, M. Lopez-Botet, M. Cella, and M. Colonna. 1996. Tyrosine phosphorylation of a human killer inhibitory receptor recruits protein tyrosine phosphatase 1C. *J. Exp. Med. 184:93.*
14. Binstadt, B. A., K. M. Brumbaugh, C. J. Dick, A. M. Scharenberg, B. L. Williams, M. Colonna, L. L. Lanier, J. P. Kinet, R. T. Abraham, and P. J. Leibson. 1996. Sequential involvement of Lck and SHP-1 with MHC-recognizing receptors on NK cells inhibits FcR-initiated tyrosine kinase activation. *Immunity 5:629.*
15. Fry, A. M., L. L. Lanier, and A. Weiss. 1996. Phosphotyrosines in the killer cell inhibitory receptor motif of NKB1 are required for negative signaling and for association with protein tyrosine phosphatase 1C. *J. Exp. Med. 184:295.*
16. Watzl, C., C. C. Stebbins, and E. O. Long. 2000. Cutting edge: NK cell inhibitory receptors prevent tyrosine phosphorylation of the activation receptor 2B4 (CD244). *J. Immunol. 165:3545.*
17. Valiante, N. M., J. H. Phillips, L. L. Lanier, and P. Parham. 1996. Killer cell inhibitory receptor recognition of human leukocyte antigen (HLA) class I blocks formation of a pp36/PLC-γ signaling complex in human natural killer (NK) cells. *J. Exp. Med. 184:2243.*
18. Binstadt, B. A., D. D. Billadeau, D. Jevremovic, B. L., Williams, N. Fang, T. Yi, G. A. Koretzky, R. T. Abraham, and P. J. Leibson. 1998. SLP-76 is a direct substrate of SHP-1 recruited to killer cell inhibitory receptors. *J. Biol. Chem. 273:27518.*
19. Jevremovic, D., D. D. Billadeau, R. A. Schoon, C. J. Dick, B. J. Irvin, W. Zhang, L. E. Samelson, R. T. Abraham, and P. J. Leibson. 1999. Cutting edge: a role for the adaptor protein LAT in human NK cell-mediated cytotoxicity. *J. Immunol. 162:2453.*

20. Kupfer, A., G. Dennert, and S. J. Singer. 1985. The orientation of the golgi apparatus and the microtubule-organizing center in the cytotoxic effector cell is a prerequisite in the lysis of bound target cells. *J. Mol. Cell Immunol. 2:37.*
21. Kupfer, A., S. J. Singer, and G. Dennert. 1986. On the mechanism of unidirectional killing in mixtures of two cytotoxic T lymphocytes: unidirectional polarization of cytoplasmic organelles and the membrane-associated cytoskeleton in the effector cells. *J. Exp. Med. 163:489.*
22. Burkhardt, J .K., S. Hester, C. K. Lapham, and Y. Argon. 1990. The lytic granules of natural killer cells are dual function organelles combining secretory and prelysosomal compartments. *J. Cell Biol. 111:2327.*
23. Griffiths, G. M., and Y. Argon. 1995. Structure and biogenesis of lytic granules. *Curr. Top, Microbiol. Immunol. 198:39.*
24. Lowin-Kropf, B., V. A. Shapiro, and A. Weiss. 1998. Cytoskeletal polarization of T cells is regulated by an immunoreceptor tyrosine-based activation motif-dependent mechanism. *J. Cell Biol. 140:861.*
25. Wei, S., D. Gilvary, B. Corliss, S. Sebti, J. Sun, D. Straus, P. Liebson, J. Trapani, A. Hamilton, M. Weber, and J. Djeu. 2000. Direct tumor lysis by NK cells uses a Ras-independent mitogen-activated protein kinase signal pathway. *J. Immunol. 165:3811.*
26. Jiang, K., B. Zong, D. Gilvary, B. Corliss, E. Hong-Geller, S. Wei, and J. Djeu. 2000. Pivotal role of phosphoinositide-3 kinase in regulation of cytotoxicity in natural killer cells. *Nat. Immunol. 1:419.*
27. Lou, Z., D. Jevremovic, D. Billadeau, and P. Leibson. 2000. A balance between positive and negative signals in cytotoxic lymphocytes regulates the polarization of lipid rafts during the development of cell-mediated killing. *J. Exp. Med. 191:347.*
28. Sancho, D., M. Nieto, M. Llano, J. L. Rodriguez-Fernandez, R. Tejedor, S. Avraham, C. Cabanas, M. Lopez-Botet, and F. Sanchez-Madrid. 2000. The tyrosine kinase PYK-2/RAFTK regulates natural killer (NK) cell cytotoxic response, and is translocated and activated upon specific target cell recognition and killing. *J. Cell Biol. 149:1249.*
29. Davis, D. M., I. Chiu, M. Fassett, G. B. Cohen, O. Mandelboim, and J. L. Strominger. 1999. The human natural killer cell immune synapse. *Proc. Natl. Acad. Sci. USA 96:15062.*
30. Eriksson, M., J. C. Ryan, M. C. Nakamura, and C. L. Sentman. 1999. Ly49A inhibitory receptors redistribute on natural killer cells during target cell interaction. *Immunology 2:341.*
31. Kupfer, A., and S. J. Singer. 1989. The specific interaction of helper T cells and antigen-presenting B cells. IV. Membrane and cytoskeletal reorganizations in the bound T cell as a function of antigen dose. *J. Exp. Med. 170:1697.*
32. Garcia, G. G., and R. A. Miller. 2001. Single-cell analyses reveal two defects in peptide-specific activation of naive T cells from aged mice. *J. Immunol. 166: 3151.*
33. Monks, C. R., H. Kupfer, I. Tamir, A. Barlow, and A. Kupfer. 1997. Selective modulation of protein kinase C-θ during T-cell activation. *Nature 385:83.*
34. Monks, C. R., B. A. Freiberg, H. Kupfer, N. Sciaky, and A. Kupfer. 1998. Three-dimensional segregation of supramolecular activation clusters in T cells. *Nature 395:82.*
35. Grakoui, A., S. K. Bromley, C. Sumen, M. M. Davis, A. S. Shaw, P. M. Allen, and M. L. Dustin. 1999. The immunological synapse: a molecular machine controlling T cell activation. *Science 285:221.*
36. Wulfing, C., and M. M. Davis. 1998. A receptor/cytoskeletal movement triggered by costimulation during T cell activation. *Science 282:2266.*
37. Viola, A., S. Schroeder, Y. Sakakibara, and A. Lanzavecchia. 1999. T lymphocyte costimulation mediated by reorganization of membrane microdomains. *Science 283:680.*
38. Dustin, M. L., and J. A. Cooper. 2000. The immunological synapse and the actin cytoskeleton: molecular hardware for T cell signaling. *Nat. Immunol. 1:23.*
39. Bi, K., Y. Tanaka, N. Coudronniere, K. Sugie, S. Hong, M.J. van Stipdonk, and A. Altman. 2001. Antigen-induced translocation of PKC-θ to membrane rafts is required for T cell activation. *Nat. Immunol. 2:556.*
40. Batista, F. D., D. Iber, and M. S. Neuberger. 2001. B cells acquire antigen from target cells after synapse formation. *Nature 411:489.*
41. Al-Alwan, M. M., G. Rowden, T. D. Lee, and K. A. West. 2001. The dendritic cell cytoskeleton is critical for the formation of the immunological synapse. *J. Immunol. 166:1452.*
42. Valiante, N. M., M. Uhrberg, H. G. Shilling, K. Lienert-Weidenbach, K. L. Arnett, A. D'Andrea, J. H. Phillips, L. L. Lanier, and P. Parham. 1997. Functionally and structurally distinct NK cell receptor repertoires in the peripheral blood of two human donors. *Immunity 7:739.*
43. Soderstrom, K., B. Corliss, L. Lanier, and J. H. Phillips. 1997. CD94/NKG2 is the predominant inhibitory receptor involved in recognition of HLA-G by decidual and peripheral blood NK cells. *J. Immunol. 159:1072.*
44. Phillips, J. H., J. E. Gumperz, P. Parham, and L. L. Lanier. 1995. Superantigen-dependent, cell-mediated cytotoxicity inhibited by MHC class I receptors on T lymphocytes. *Science 268:403.*
45. Einspahr, K. J., R. T. Abraham, B. A. Binstadt, Y. Uehara, and P. J. Leibson. 1991. Tyrosine phosphorylation provides an early and requisite signal for the activation of natural killer cell cytotoxic function. *Proc. Natl. Acad. Sci. USA 88:6279.*
46. Brumbaugh, K. M., B. A. Binstadt, D. D. Billadeau, R. A. Schoon, C. J. Dick, R. M. Ten, and P. J. Leibson. 1997. Functional role for Syk tyrosine kinase in natural killer cell-mediated natural cytotoxicity. *J. Exp. Med. 186:1965.*
47. Ting, A. T., C. J. Dick, R. A. Schoon, L. M. Karnitz, R. T. Abraham, and P. J. Leibson. 1995. Interaction between lck and syk family tyrosine kinases in Fcγ receptor-initiated activation of natural killer cells. *J. Biol. Chem. 270:16415.*
48. Vyas, Y., A. Selvakumar, U. Steffens, and B. Dupont. 1998. Multiple transcripts of the killer cell immunoglobulin-like receptor family, KIR3DL1 (NKB1) are expressed by NK cells of a single individual. *Tissue Antigens 52:510.*
49. Callewaert, D. M., G. Radcliff, R. Waite, J. LeFevre, and M. D. Poul. 1991. Characterization of effector-target conjugates for cloned human natural killer and human lymphokine activated killer cells by flow cytometry. *Cytometry 12:666.*
50. Peterson, E. J., J. L. Clements, Z. K. Ballas, and G. A. Koretzky. 1999. NK cytokine secretion and cytotoxicity occur independently of the SLP-76 adaptor protein. *Eur. J. Immunol. 29:2223.*
51. Ishiai, M., M. Kurosaki, K. Inabe, A. C. Chan, K. Sugamura, and T. Kurosaki. 2000. Involvement of LAT, Gads, and Grb2 in compartmentation of SLP-76 to the plasma membrane. *J. Exp. Med. 192:847.*
52. Blery, M., J. Delon, A. Trautmann, A. Cambiaggi, L. Olcese, R. Biassoni, L. Moretta, P. Chavrier, A. Moretta, M. Daeron, et al. 1997. Reconstituted killer cell inhibitory receptors for major histocompatibility complex class I molecules control mast cell activation induced via immunoreceptor tyrosine-based activation motifs. *J. Biol. Chem. 272:8989.*
53. Boerth, N. J., J. J. Sadler, D. E. Bauer, J. L. Clements, S. M. Gheith, and G. A. Koretzky. 2000. Recruitment of SLP-76 to the membrane and glycolipid-enriched membrane microdomains replaces the requirement for linker for activation of T cells in T cell receptor signaling. *J. Exp. Med. 192:1047.*
54. Bunnell, S. C., M. Diehn, M. B. Yaffe, P. R. Findell, L. C. Cantley, and L. J. Berg. 2000. Biochemical interactions integrating Itk with the T cell receptor-initiated signaling cascade. *J. Biol. Chem. 275:2219.*
55. Sun, Z., C. W. Arendt, W. Ellmeier, E. M. Schaeffer, M. J. Sunshine, L. Gandhi, J. Annes, D. Petrzilka, A. Kupfer, P. L. Schwartzberg, et al. 2000. PKC-θ is required for TCR-induced NF-κB activation in mature but not immature T lymphocytes. *Nature 404:402.*
56. Viola, A., S. Schroeder, Y. Sakakibara, and A. Lanzavecchia. 1999. T lymphocyte costimulation mediated by reorganization of membrane microdomains. *Science 283:680.*
57. Parolini, I., M. Sargiacomo, M. P. Lisanti, and C. Peschle. 1996. Signal transduction and glycophosphatidylinositol-linked proteins (*lyn*, *lck*, CD4, CD45, G proteins, and CD55) selectively localize in Triton-insoluble plasma membrane domains of human leukemic cell lines and normal granulocytes. *Blood 87:3783.*
58. Su, M. W., C. L. Yu, S. J. Burakoff, and Y. J. Jin. 2001. Targeting Src homology 2 domain-containing tyrosine phosphatase (SHP-1) into lipid rafts inhibits CD3-induced T cell activation. *J. Immunol. 166:3975.*
59. Trotta, R., K. Fettucciari, L. Azzoni, B. Abebe, K. A. Puorro, L. C. Eisenlohr, and B. Perussia. 2000. Differential role of p38 and c-Jun N-terminal kinase 1 mitogen-activated protein kinases in NK cell cytotoxicity. *J. Immunol. 165:1782.*
60. Lowin-Kropf, B., B. Kunz, F. Beermann, and W. Held. 2000. Impaired natural killing of MHC class I-deficient targets by NK cells expressing a catalytically inactive form of SHP-1. *J. Immunol. 165:1314.*
61. Burshtyn, D. N., J. Shin, C. Stebbins, and E. O. Long. 2000. Adhesion to target cells is disrupted by the killer cell inhibitory receptor. *Curr. Biol. 10:777.*
62. Kong, G. H., J. Y. Bu, T. Kurosaki, A. S. Shaw, and A. C. Chan. 1995. Reconstitution of Syk function by the ZAP-70 protein tyrosine kinase. *Immunity 2:485.*
63. Wong, J., M. Ishiai, T. Kurosaki, and A. C. Chan. 2000. Functional complementation of BLNK by SLP-76 and LAT linker proteins. *J. Biol. Chem. 275:33116.*
64. Fu, C., C. W. Turck, T. Kurosaki, and A. C. Chan. 1998. BLNK: a central linker protein in B cell activation. *Immunity 9:93.*
65. Bonilla, F. A., R. M. Fujita, V. I. Pivniouk, A. C. Chan, and R. S. Geha. 2000. Adapter proteins SLP-76 and BLNK both are expressed by murine macrophages and are linked to signaling via Fcγ receptors I and II/III. *Proc. Natl. Acad. Sci. USA 97:1725.*
66. Eriksson, M., G. Leitz, E. Fallman, O. Axner, J. C. Ryan, M. C. Nakamura, and C. L. Sentman. 1999. Inhibitory receptors alter natural killer cell interactions with target cells yet allow simultaneous killing of susceptible targets. *J. Exp. Med. 190:1005.*
67. Wulfing, C., M. D. Sjaastad, and M. M. Davis. 1998. Visualizing the dynamics of T cell activation: intracellular adhesion molecule 1 migrates rapidly to the T cell/B cell interface and acts to sustain calcium levels. *Proc. Natl. Acad. Sci. USA 95:6302.*
68. Azuma, M., M. Cayabyab, D. Buck, J. H. Phillips, and L. L. Lanier. 1992. Involvement of CD28 in MHC-unrestricted cytotoxicity mediated by a human natural killer leukemia cell line. *J. Immunol. 149:1115.*
69. Teng, J. M., X. R. Liu, G. B. Mills, and B. Dupont. 1996. CD28-mediated cytotoxicity by the human leukemic NK cell line YT involves tyrosine phosphorylation, activation of phosphatidylinositol 3-kinase, and protein kinase C. *J. Immunol. 156:3222.*